



UNIVERSITÀ  
DEGLI STUDI  
FIRENZE

# FLORE

## Repository istituzionale dell'Università degli Studi di Firenze

### **Experimental study of the wind pressure field on the Notre Dame Cathedral in Paris**

Questa è la Versione finale referata (Post print/Accepted manuscript) della seguente pubblicazione:

*Original Citation:*

Experimental study of the wind pressure field on the Notre Dame Cathedral in Paris / Claudio Mannini, Tommaso Massai, Enrico Panettieri, Niccolo' Barni, Andrea Giachetti, Margherita Ferrucci, Marco Montemurro, Paolo Vannucci. - In: INTERNATIONAL JOURNAL OF ARCHITECTURAL HERITAGE. - ISSN 1558-3066. - STAMPA. - 18:(2024), pp. 194-214. [10.1080/15583058.2022.2136022]

*Availability:*

The webpage <https://hdl.handle.net/2158/1283459> of the repository was last updated on 2025-11-02T11:17:10Z

*Published version:*

DOI: 10.1080/15583058.2022.2136022

*Terms of use:*

Open Access

La pubblicazione è resa disponibile sotto le norme e i termini della licenza di deposito, secondo quanto stabilito dalla Policy per l'accesso aperto dell'Università degli Studi di Firenze (<https://www.sba.unifi.it/upload/policy-oa-2016-1.pdf>)

*Publisher copyright claim:*

La data sopra indicata si riferisce all'ultimo aggiornamento della scheda del Repository FloRe - The above-mentioned date refers to the last update of the record in the Institutional Repository FloRe

(Article begins on next page)

# Experimental study of the wind pressure field on the Notre Dame Cathedral in Paris

Claudio Mannini<sup>1</sup>, Tommaso Massai<sup>1</sup>, Enrico Panettieri<sup>2</sup>, Niccolò Barni<sup>1</sup>, Andrea Giachetti<sup>1</sup>,  
Margherita Ferrucci<sup>3</sup>, Marco Montemurro<sup>2</sup>, and P. Vannucci<sup>\*4</sup>

<sup>1</sup>CRIACIV-Department of Civil and Environmental Engineering, University of Florence,  
Via S. Marta, 3, 50139 Florence, Italy

<sup>2</sup>Arts et Métiers Institut of Technology - Université de Bordeaux, CNRS, INRA, Bordeaux INP,  
HESAM Université, I2M UMR5295, 33405 Talence, France.

<sup>3</sup>Laboratorio di Fisica Tecnica Ambientale, Università IUAV, 30135 Venezia, Italy.

<sup>4</sup>LMV - UMR8100, Université Paris-Saclay - UVSQ. 45, Avenue des Etats-Unis,  
78035 Versailles, France.

August 31, 2022

---

## Abstract

The paper concerns an experimental study on the wind pressures over the surface of a worldwide known Gothic Cathedral: Notre Dame of Paris. The experimental tests have been conducted in the CRIACIV wind tunnel, Prato (Italy), on a model of the Cathedral at the scale 1:200 reproducing the atmospheric boundary layer. Two types of tests have been conducted: with or without the surrounding modeling the part of the city of Paris near the Cathedral. This has been done, on the one hand, for evaluating the effect of the surrounding buildings onto the wind pressure

---

<sup>\*</sup>Corresponding author: [paolo.vannucci@uvsq.fr](mailto:paolo.vannucci@uvsq.fr)

distribution on the Cathedral, and, on the other hand, to have a wind pressure distribution plausible for any other Cathedral with a similar shape. The tests have been done for all the wind directions and the mean and peak pressures have been recorded. The results emphasize that the complex geometry of this type of structures is responsible for a peculiar aerodynamic behavior that does not allow estimating correctly the wind loads on the various parts of the Cathedral based on codes and standards, which are tailored for ordinary regular buildings.

**Key words:** Gothic Cathedral, Notre Dame, wind pressure, wind tunnel tests, climate change effects, additive manufacturing.

---

## 1 Introduction

The scientific research on built heritage is more and more pushed by environmental problems, such as the climate change (Orr et al. 2021), which represents an increasing threat for its preservation. Some recent, still ongoing, research projects testify of the importance of the relationship between built heritage and climate change and of the increasing interest of governments, supranational organizations, conscious that the conservation of the architectural heritage is linked to the fundamental values of the social and intellectual life of the nations (Deland et al. 2020). We recall, for instance, the projects funded by the European Union within the Joint Programming Initiative on Cultural Heritage and Global Change and by the Cultural Heritage H2020-EU<sup>1</sup>. In particular, the global warm-

---

<sup>1</sup>HYPERION (Development of a Decision Support System for Improved Resilience and Sustainable Reconstruction of historic areas to cope with Climate Change and Extreme Events based on Novel Sensors and Modelling Tools);

ARCH (Advancing Resilience of Historic Areas against Climate-related and other Hazards);

CONSECH20 (CONSErvation of 20th century concrete Cultural Heritage in urban changing environments).

ing of Earth is causing more and more frequent and strong wind storms, which constitute today (and will constitute) a severe threat for the conservation of some iconic monumental structures. According to [Steenbergen et al. \(2012\)](#), the climate change implies an increase up to 2.3% in the hourly mean wind speed with a return period of 50 years. An adequate evaluation of the wind pressure on monumental structures is hence of paramount importance for a correct safety evaluation of such structures in the next future.

This is even more stringent for high-rise buildings, like the Gothic Cathedrals, which are more exposed to the action of wind, whose speed increases with the height above the ground. An example of the increasing danger such monuments are exposed to, is the damage to the great rose of the Cathedral of Soissons (France), destroyed by the storm Egon on January 13th, 2017. Some minor damages were also suffered by other great Gothic Cathedrals in France during the severe wind storms of the last days of December 1999, like the Notre Dame Cathedral in Paris, where a wind as strong as 169 km/h was recorded inside the city. Famous is also the collapse of the Spire of Saint Bonifatius Church in Leeuwarden, The Netherlands, during a wind storm in 1976. To this end, this paper focuses on the evaluation of wind pressures on Gothic Cathedrals, which are a major example of the built heritage in Europe.

Generally, four approaches are used to investigate the wind effects on structures in the atmospheric boundary layer: theoretical studies, full-scale measurements, Computation Fluid Dynamics (CFD) numerical simulations and physical experiments on reduced-scale models. Theoretical models concern objects of simple, aerodynamic shape, and they are not suited for complex structures like Gothic Cathedrals. Full-scale measurements are very expensive and require the possibility of equipping with sensors the considered structure. For these reasons, in wind engineering experimental campaigns *in situ* are



still scarce and often they serve to corroborate either the results of experiments on scale models or the results of a computation. CFD numerical simulations are more and more used in the study of the wind pressure and velocity fields around buildings. Although they can provide detailed information on the relevant flow variables, their accuracy and reliability are still of concern, especially when the simulations regard buildings with a complicated shape, located in an urban environment, as in the case of Gothic Cathedrals. In such situations, the validation of the studies by full-scale measurements or reduced-scale experimental tests is necessary (Blocken 2014). Therefore, experiments on scale physical models in wind tunnels, used since the early twentieth century (Ferrucci and Peter 2020) remain still today an indispensable and reliable tool for a correct analysis of the wind field around buildings of complicated geometry in an urban landscape.

Due to their dimensions and geometry, the fine detail and richness of their decorations, their particular structural organization, composed by high vaults, flying buttresses, timber roofing, and also due to the materials they are composed of (i.e., stone, mortar, stain-glasses, wood), Gothic Cathedrals are very peculiar and quite delicate structures. The use of some technical norms, e.g. Eurocode 1 (CEN 2004), in evaluating the wind load on them, seems inadequate. Indeed, such norms are conceived for the design of ordinary new buildings, while Gothic Cathedrals are existing and really extra-ordinary constructions. In particular, the wind load prescribed by Eurocode 1 is very simplified and, for a complicated structure, it is not possible to know whether it over- or under-estimates the real loading. Therefore, it would be pretentious and rather unrealistic to assess the structural safety of a Gothic Cathedral, in respect of the increasingly severe wind storms that are caused by climate change, using so a rough model. Indeed, a deep scientific investigation of the wind-induced pressure distribution on the surface of a Gothic Cathedral is necessary for

a correct risk assessment of such structures or of some parts of them. This is a scientific challenge that still waits for an adequate response.

In the literature, experimental studies of the wind pressure field on a Cathedral, even if not Gothic, are rare. A few works focus on the spires of Cathedrals, or on slender structures similar to spires, or on masonry structures of particular value or architectural interest; some of them are briefly recalled hereafter. To the authors' best knowledge, there is only an old wind tunnel investigation on a bi-dimensional model of a Cathedral-like building (Chien et al. 1951). Originally, this study did not concern Cathedrals or churches in particular, but just buildings with some typical cross-section shapes, one of them being similar to a simple model of the nave of a Middle Age church. Results were given in the form of bi-dimensional diagrams of the wind pressure coefficient, as shown in Fig. 1, and it has been the basis for some subsequent pioneer works on the matter made by R. Marks and co-workers, e.g. Mark and Jonash (1970). Two studies on the dynamic response of two slender masonry structures to wind actions, the San Gaudenzio Basilica in Novara and the Mole Antonelliana in Turin (both in Italy), are cited in Calderini and Pagnini (2015). For the latter, a storm caused the collapse of the spire in 1953, and its reconstruction was undertaken only after wind tunnel tests in the Aeronautics Laboratory of the Turin Polytechnic University in 1954. The wind pressure on the Church of Sainte-Jeanne-d'Arc in Rouen (France) was determined by wind tunnel experiments in the Eiffel Laboratory in Paris (Romani 1972). In Szalay (1983), a wind tunnel study for a damaged ancient church spire is proposed, in order to evaluate the wind load to be used for the design of the reinforcing structure. The experiments were performed in the Hungarian Institute of Building Science. The investigation about the wind effects on the leaning Tower of Pisa (Italy) is described in Solari et al. (1998). The experiments were devoted to understand

the wind load that could cause the collapse of the tower due to the weak strength of the foundation soil. The wind-induced pressures on the monumental roof structure of the XII century Palazzo della Ragione in Padova were also experimentally studied in [Borri and Facchini \(1999\)](#). The tests were performed in the CRIACIV wind tunnel Laboratory in Prato (Italy). More recently, in a study on the vulnerability of the Capetian architecture to wind storms ([Brocato et al. 2016](#)), CFD simulations were carried out on 2D simplified models of some churches. In [Domede et al. \(2019\)](#), the wind load provided by Eurocode 1 is compared to the ancient methods available at the time of the construction (end of XIX century) of the Ile Vierge Lighthouse (France), the tallest stone lighthouse in Europe.

As far as Gothic Cathedrals are specifically concerned, there are very few studies on the wind actions: this is rather surprising, being these structures sensitive to wind storms due to their height and large dimensions. Usually, the structure of the Cathedral is modeled through a simple bi-dimensional scheme and analyzed with different techniques: the line of pressure method in [Ungewitter \(1890\)](#); photo-elasticity in [Mark and Jonash \(1970\)](#), [Mark \(1982; 1984\)](#); limit analysis in [Como \(2013\)](#) and [Coccia et al. \(2015\)](#). The only work on the wind strength of a Gothic Cathedral considering a three-dimensional, though partial, model and a nonlinear material behavior is a recent paper ([Vannucci et al. 2019](#)). Just as an example, Fig. 1 shows the wind load on a Cathedral-like construction as suggested in [Chien et al. \(1951\)](#) and how this is applied to a bi-dimensional Cathedral model in [Mark and Jonash \(1970\)](#). In all of the works cited above, the wind pressure is simply modeled as a uniform or linearly variable load. Also in a recent study about the roofing structure of Notre Dame in Paris, destroyed by the fire of April 15th, 2019, the wind load is assumed as step-wise uniform ([Vannucci 2021](#)).

The present work is an experimental study that aims at providing an extensive evalu-

134 ation of the wind load that can be expected on the various parts of a Gothic Cathedral.  
135 Such a study is clearly still missing in the literature, and without any doubt it is a fun-  
136 damental step for a correct evaluation of the structural safety of such monuments. The  
137 experimental investigation is carried out in a boundary-layer wind tunnel on a physical  
138 scale model of the Cathedral of Notre Dame in Paris, an emblematic building of the French  
139 Gothic age.

140 The goal of the present study is twofold. Firstly, it aims at providing a precise portrait  
141 of the wind pressure field on this iconic construction, which has been the objective of many  
142 discussions and structural analyses after the infamous recent fire that destroyed the roof,  
143 the spire and damaged parts of the vaults. Secondly, regarding the assessment of the  
144 wind effects, Notre Dame in Paris can be seen as a sort of paradigm of a more generic  
145 Gothic Cathedral. Thus, an emphasis is put on the influence of the specific surrounding  
146 built environment on the pressure field and, by consequence, the tests are made with or  
147 without the surrounding city environment.

148 It is worth noting that this experimental study is performed not only on an extremely  
149 precise physical model of the Cathedral, realized through 3D-printing, but also, and this  
150 constitutes a scientific primacy, on a highly instrumented model. Thanks to a careful and  
151 very dense distribution of pressure captors, a fine reconstruction of the wind load on the  
152 various parts of a Gothic Cathedral has thus been possible for the first time.

## 2 Fabrication technology and materials of the Cathedral's model

The campaign of experimental tests has been done on a physical model of the Cathedral at the scale of 1:200. This scale has been chosen accounting for the dimensions of the Cathedral (130 m long, 45 m wide, 44 m high at the roof's top and 96 m at the spire's top) in order to satisfy a number of requirements. On the one hand, the model should be as large as possible to allow for a finer reproduction of the complex geometry of the structure and to facilitate the installation of a large number of pressure taps in all of its parts (see Section 2.2). On the other hand, the model must be “small” compared to the wind tunnel test chamber (2.4 m wide and 1.6 m high in the present case) not to alter the flow field around the construction (blockage effect). The generally accepted rule of the thumb is that the area of the blocking obstacle projected in a plane perpendicular to the flow is less than 5% of the wind tunnel test section. However, the most cogent physical limitation is often represented by the scale at which it is possible to reproduce in the wind tunnel the target wind flow characteristics (see Section 3.4), which must be scaled in the same way as the model of the Cathedral. Finally, the model used is 65 cm long, 22.5 cm wide, 22 cm high (top of the roof), and the spire is 48 cm high.

The model has been conceived as rigid, as a Gothic cathedral is very massive and poorly deformable, hence no aeroelastic phenomena are to be expected.

### 2.1 Fabrication technology

The realization of the physical scale model of Notre Dame was conditioned by some technological requirements. First, in order to have reliable experimental results, the model

must reproduce the geometry of the Cathedral with a high fidelity. This is quite a hard task for a building like a Gothic Cathedral, which has a complex form and is rich of details, like pinnacles, sculptures, etc. Then, the model must be instrumented with a large number of pressure taps, cf. Section 2.2, placed everywhere over the surface of the model. For these reasons, the model was fabricated using the 3D-printing technology, that enables manufacturing possibilities which cannot be achieved through classical processes, cf., e.g., Ngo et al. (2018), Wang et al. (2017), Mitchell et al. (2018), Cano-Vicent et al. (2021). In particular, it is possible to realize objects not only with very complex shapes, but also composed of different materials. Due to the dimensions and the geometrical complexity of the Notre Dame Cathedral model, the FDM (Fused Deposition Modeling) technology was chosen, except for those regions of the Cathedral characterized by very fine details, e.g., the spire, manufactured via the SLA printing technology (stereolithography) and assembled afterwards.

## 2.2 Model preparation, fabrication and materials

The model of the Cathedral has been fabricated starting from an existing high-fidelity numerical mock-up (MiniWorld3D 2019). However, the numerical model has been thoroughly modified in order to obtain a physical model of the Cathedral at the scale of 1:200 well adapted to the wind tunnel tests, and to comply with the specificity of the FDM printing technology. In fact, the physical model had to be equipped with many pressure captors and it had to allow the different manipulations needed in the laboratory for the set up of the experiment. Also, some modifications have been done on the original numerical model in order to minimize the volume of material and the printing time. The 3D computer graphics software Blender (Blender Online Community 2021), has been used to

work on the numerical model of the Cathedral.

The modifications have been carried out directly on the STL (Standard Tessellation Language) file by means of boolean operations or via adjustments of the initial mesh. In order to be able to place all of the 1200 flexible tubes that connect the holes on the model surface to the pressure sensors, the walls of the model have been modified on the internal side through the subtraction of a cone, so as to be possible to place the tubes in the holes. This rather complicated operation has been made on the numerical model using a python script coupled with Blender, modifying the file by some boolean operations. The holes for the pressure taps have also been printed, though in a second moment these have been rectified with a mini-drill in the wind tunnel.

The spire, which is rich in extremely fine details, has been fabricated using a more precise numerical model (3D Warehouse 2014), and a 3D printer based upon the SLA technology, that allows to obtain extremely precise objects, also when of very complicated shape. The model of the spire so obtained has then been assembled with the Cathedral.

The whole model, Cathedral plus spire, is composed of 15 parts, separately fabricated and then assembled together. This has been done for two reasons: the limits of the printers (maximum height: 600 mm; maximum width: 390 mm) and the need of working on the model for installing the many pressure captors. The different parts have been assembled using magnets and bolts. A scheme of the parts of the model, some details of it, showing also the holes for the captors, and the final physical model are shown in Fig. 2.

The 3D printing of the Cathedral mock-up was performed at the ENSAM facilities in Bordeaux by means of a Lynxter S600D 3D printer (Lynxter 2021), equipped with a single extrusion filament tool-head, selected in the light of its large building volume and its excellent printing performance.

The 3D printing made use of white PolyMax™PLA filament that, thanks to its nano-reinforcement technology, represents a suitable compromise between ease and quality of printing and acceptable mechanical stiffness. The Simplify3D slicing software (Simplify3D 2021), was used to prepare the G-code files used by the printing machine. The total printing time was about two weeks.

## 2.3 The surrounding environment

The mock-up of the buildings constituting the surrounding of the Cathedral has been obtained by combining data from two sources: an existing STL file of the center of Paris, cf. the website 3D CAD browser (2021), and 3D data extracted from the OpenStreetMap database (OpenStreetMap 2017).

For the purposes of the wind tunnel tests, it was sufficient to realize buildings having simplified shapes but correct (scaled) heights. The blocks of buildings constituting the surrounding model are shown in Fig. 3(a).

Because of the significant total volume of the buildings and their simple shapes, the model of the surrounding has been fabricated using wood plates, through a milling machine used to cut plates complying with the planforms of the buildings. An example of a planform of an array of buildings is shown in Fig. 3(b). For a generic building, the final height was obtained by simply stacking up and gluing together the milled wood plates.

Finally, the wind tunnel floor was lifted up of 4 cm, so to simulate the presence of the Seine River, being the distance between the base of the Cathedral and the average water level about 8 m at full scale. A view of the complete test set-up, with the models of the Cathedral and the surrounding on the turning table of the wind tunnel is shown in Fig. 3(c).



## 3 Experimental campaign

### 3.1 General outline

To determine the wind pressure field over the whole external surface of the Cathedral, the physical model of Notre Dame has been equipped with 1200 pressure gauges, whose distribution has been studied in order to obtain, by interpolation methods, detailed charts of the pressure coefficients, cf. Section 4. As previously said, the study has been conducted on the Cathedral model with and without the surrounding parts of Paris, see Fig. 4. This, for two reasons: on the one hand, to evaluate the influence of the surrounding buildings and, on the other hand, for obtaining pressure coefficient distributions that can represent the wind loading on similar buildings immersed in a generic urban wind profile (considering Notre Dame as a sort of Gothic Cathedral archetype). In both cases, the wind profile has been generated through artificial roughness elements, cf. Section 3.4. The test campaign has been carried out recording the pressure on the surface of the Cathedral for many different wind directions, according to the scheme presented in Fig. 5. Therein, the orientation of the Cathedral with respect to the canonical geographical directions, the wind tunnel azimuths and the surrounding buildings can be seen. The direction denoted as  $0^\circ$  (West-Northwest) is perpendicular to the main façade, while  $90^\circ$  means that the wind blows perpendicularly to the naves from the side where the neighboring buildings are closer to the Cathedral (North-Northeast). A wind direction of  $270^\circ$  indicates a wind perpendicular to the naves but coming from the South-Southwest side.

## 3.2 Wind tunnel facility

The tests were carried out in the open-circuit boundary layer wind tunnel of CRIACIV<sup>2</sup> in Prato, Italy. The facility is 22 m long and presents at the inlet a nozzle with a contraction ratio of 3 to 1 after the honeycomb and a T-diffuser at the outlet. The test chamber is 1.6 m high, while the width varies from 2.2 m after the nozzle to 2.4 m at the position of the turning table. The latter has a diameter of 2.2 m. The overall length of the fetch to develop boundary layer flows is about 11 m. Air is drawn by a motor with a nominal power of 156 kW, and the flow speed can be varied continuously up to about 30 m/s by adjusting through an inverter the rotation speed of the fan or the pitch of its ten blades. In the absence of turbulence generating devices, the free-stream turbulence intensity is less than 1%.

## 3.3 Model equipment

The model of the Cathedral has been equipped with Teflon tubes with an internal diameter of 1 mm, used to connect the taps on the model surface with the pressure sensors, see Fig. 6. The tubes were 30 cm long, obtained by linking two pieces having the same internal diameter with a short restrictor tube of about 1 cm working as a damper (see e.g. Irwin et al. (1979)). Such pneumatic connections have been calibrated beforehand to guarantee an acceptably flat transfer function in the frequency range of interest (up to about 200 Hz in the present case) (see e.g. Holmes (2007)).

Due to the limited number of pressure sensors available, groups of 222 pressure taps were simultaneously recorded at a sampling rate of 500 Hz with the system PSI DTC

---

<sup>2</sup>Centro di Ricerca Interuniversitario di Aerodinamica delle Costruzioni e Ingegneria del Vento, Inter-University Research Centre on Building Aerodynamics and Wind Engineering

Initium. The restriction on the number of simultaneous signals logged is not an issue if the mean pressures are concerned, but it must be borne in mind if the resultant load on specific parts of the structure is calculated; indeed, the partial correlation of pressure fluctuations has to be taken into account in this case. For this reason, the groups of pressure taps have been chosen based on the structural macro-elements of the Cathedral. The accuracy of the piezoelectric sensors of the 32-port miniaturized ESP-32HD pressure scanners is  $\pm 2.45$  Pa. Each signal was recorded for about 120 s at a reference mean wind speed of about 19.5 m/s at the top of the Cathedral roof.

At full scale, following the Eurocode 1 (CEN 2004), a mean wind speed of 21.3 m/s is expected at a height of 44 m (top of the roof) for a terrain category IV (urban profile) and a return period of 50 years. Consequently, the velocity scale of the tests is about 1:1.1, while the time scale results to be about 1:183. This means that a sampling frequency of 500 Hz allows detecting pressure fluctuations at full scale up to a frequency of about 1.37 Hz, thus encompassing the most energetic atmospheric turbulent fluctuations. Moreover, 120 s at laboratory scale correspond to 21960 s at full scale, that is more than 36 time windows of 10 minutes, which is suitable to calculate the statistics of the peak values of pressures in compliance with Eurocode 1 (see also Section 4.2).

### 3.4 Oncoming flow

For the city centre of Paris, the previously mentioned turbulent wind profile associated with the terrain category IV of Eurocode 1 has been assumed for all azimuthal directions. The atmospheric boundary layer flow at the same scale of the model (1:200) has been reproduced through artificial roughness elements of variable size diffused all over the floor of the test chamber. A castellated barrier, placed at the inlet section of the wind tunnel

has also been employed to increase the turbulence intensity.

Fig. 7 shows the modeled wind characteristics in the wind tunnel at the beginning of the turning table, slightly upstream of the model of the Cathedral. Flow velocity measurements were carried out with a single-component hot-wire anemometer recorded at a sampling rate of 10 kHz. The mean wind velocity pattern is in very good agreement with the assumed target urban profile (Fig. 7(a)). The longitudinal turbulence intensity, which is a normalized integral measure of the wind velocity fluctuations (a coefficient of variation, indeed), is slightly lower than the Eurocode 1 target (Fig. 7(b)). The longitudinal integral length scale of turbulence, which represents the correlation length of the wind velocity fluctuations along the mean velocity direction and rules the frequency distribution of the turbulent kinetic energy in the stream (see e.g. Simiu and Yeo (2019)), closely follows the target pattern up to about 30 m above the ground; afterwards, the increase with the height becomes slower than in the Eurocode 1 profile (Fig. 7(b)). However, the discrepancy is moderate at least up to the top of the Cathedral roof. Finally, Fig. 7(d) shows that the spectral characteristics of the generated boundary layer comply very well with a von Kármán-Harris spectrum, which is very often assumed to describe the energy cascade of turbulence, Simiu and Yeo (2019). Measurements have also been carried out to assess the homogeneity of the flow in the transversal and longitudinal directions.

In general, despite the large scale of the model with respect to the present wind tunnel facility, we can conclude that the modeled turbulent wind is well representative of an urban environment such as the one that can be expected in the centre of Paris.

As said above, two different configurations of the model have been tested. In the first one, the turning table was covered with roughness elements of progressively reduced height close to the Cathedral model (cf. Fig. 4(a)), in order to transfer the same generic

urban wind profile from the beginning of the turning table to the model position and beyond. In contrast, the second configuration includes the model of the surrounding of the Cathedral, as shown in Fig. 4(b).

## 4 Results of the experimental tests

The results of pressure measurements on the external surface of the Cathedral are reported in this section in the form of pressure coefficients, defined as follows:

$$C_p = \frac{p - p_0}{\frac{1}{2}\rho V^2(z_{ref})}, \quad (1)$$

where  $p$  is the pressure on the considered point of the structure,  $p_0$  is the static pressure of the undisturbed flow in the wind tunnel at the position of the model,  $\rho$  is the air density and  $V(z_{ref})$  is the reference wind speed, that is the mean flow velocity at the top of the roof ( $z_{ref} = H = 44$  m at full scale) in the absence of the model (see the mean wind velocity profile in Fig. 7(a)). It is noteworthy that the accuracy of the pressure transducers, given the reference velocity pressure in the tests, corresponds to  $\pm 0.01$  in terms of  $C_p$ . The recorded data can be divided in mean pressure and gust pressure data. The former are simply calculated as the time averages of the recorded pressure coefficients. The latter are defined as the average of either the maximum or the minimum values of  $C_p$  registered over full-scale time windows of 10 minutes (see Section 4.2). The results are reported hereafter in terms of pressure coefficient charts, obtained by linear interpolation and heuristically controlled extrapolation of the measured values. The small black spots indicate the taps where pressure was actually measured.

## 4.1 Mean pressure charts

Fig. 8 gives the global distribution of the pressure coefficients on the lateral side of the Cathedral in the presence of the surrounding model and wind coming from the 90°-direction. It is worth noting the strong pressure gradient in correspondence of the windward rose of the transept and the large pressure coefficients in the higher part of the transept ( $C_p > 0.9$ ).

The pressure coefficient distribution over the front of the Cathedral is reported in Fig. 9 for a wind perpendicular to it (0°-direction). It is apparent that the particular geometry of the towers produces large pressure gradients close to the edges of the façade. It is also noteworthy that values of  $C_p$  larger than unity can be found in the upper part of the towers; this is because the reference velocity pressure is taken at a lower height, that is that of the top of the roof (see Eq. (1)).

Mean pressure coefficient charts are presented in Fig. 10 also for the apse, for a wind blowing either from the direction perpendicular to the left flank (90°) or parallel to the longitudinal axis of the Cathedral (180°). In the former case, one can notice a strong pressure gradient due to the curvature of the walls, which from positive pressure coefficients around 0.35 on the windward side quickly leads to strong suctions (up to  $C_p \cong -0.8$ ) in the middle upper part. In contrast, for a wind direction of 180° positive mean pressure coefficients up to about 0.8 are attained in the central upper portion of the apse. In the lower part of the left side of the apse (bottom right corner in Fig. 10(a) and 10(b)), one can also remark the effect of the surrounding buildings, which are very close to the apse. They shelter the flank of the Cathedral from direct wind for an azimuth angle of 90°, while they promote a flow acceleration, and then a pressure decrease, for a wind direction of 180°.

#### 4.1.1 Detail of the flank

A lateral portion of the Cathedral between the front and the transept (indicated in red in Fig. 5) has been very densely instrumented, in order to have more details of the pressure coefficient distribution through the height of the Cathedral on a representative part of it. Results are shown in Fig. 11. In the case of a generic urban profile (i.e., without surrounding, Fig. 11(a)), pressure coefficients between about 0.6 and 0.75 are found on the windward walls. However, the most interesting features can be observed on the windward side of the roof, where a bubble of high pressure (with mean pressure coefficients up to about 0.55) is apparent in the central part. This is due to the flow acceleration on the upper side of the roof (with consequent decrease of pressure) and the strong inclination of the flow that locally separates at the balustrade at the base of the roof. Flow visualizations with a smoke generator (Fig. 12) revealed that this is also due to the significant vertical wind component induced by the three orders of walls on the flank of the Cathedral. On the leeward side, the pressure is nearly uniform, with mean  $C_p$  values between about  $-0.45$  and  $-0.4$ .

Fig. 11 clearly shows how the presence of the buildings upstream of the Cathedral and very close to it affects the load distribution. The pressure remarkably decreases on the lower part of the windward walls due to the sheltering effect of the neighboring buildings (in some regions, the pressure coefficients even pass from about 0.6 to about 0.2), but the vertical wind velocity component also reduces, producing a slight increase of the mean  $C_p$  on the upper portion of the windward wall and a pronounced increment on the roof (of the order of 20-25% but even higher at the base of the roof, behind or just above the balustrade). An increase of pressure between about 10 and 25% can also be observed on the leeward side of the Cathedral (lower suction).

### 4.1.2 Roof

The results discussed in the previous section are confirmed by Fig. 13, which reports the pressure distribution on the entire roof of the Cathedral. It can be remarked that, despite the roof is at a significantly greater height than the surrounding buildings, the presence of the latter has a remarkable impact on the pressure distribution over it, as previously said, probably accelerating the upper flow and reducing the vertical component of the velocity with which the wind attacks the windward pitch of the roof. Indeed, while the pressure coefficient hardly attains 0.57 in a small windward region between the façade and the transept when the surrounding buildings are not reproduced, it overcomes 0.7 at several locations if the latter are in place.

## 4.2 Peak loads

For the local design or verification of cladding elements or secondary structures, and also to have a statistical measure of the fluctuation of pressures, peak values can be calculated according to Davenport (1961)'s approach, i.e. as the average of maxima (or minima) associated with a given observation time (600 s according to Eurocode 1's approach). Given the time scale of the current experiments, as said in Section 3.3, the length of the recorded signals corresponds to about 36 windows of 10 minutes at full scale and allows a statistically meaningful calculation of wind load peak values. Moreover, to be representative of area-averaged pressures, the maxima (or minima) are calculated on time records filtered via a moving average over a set time window (Lawson 1976, Holmes 1997). In the present analysis, the classical full-scale window of 1 s has been chosen.

Fig. 14 shows the distribution of the maximum pressure coefficients on the North-Northeast flank of the Cathedral for a wind perpendicular to the walls (90°-direction).



Large values of the load can be observed due to wind gusts, the  $C_p$  chart showing values even beyond 2. The higher peak pressures are obtained just above the big rose window of the transept façade. The comparison with Fig. 8(a) shows that high gust factors (ratio of maximum to mean value of pressures) mostly between about 2.4 and 4 are obtained.

The comparison of Fig. 14(a) and Fig. 14(b) emphasizes the effect of the surrounding buildings around the Cathedral on the peak pressure coefficients. Coherently with the observations already done for the mean pressures (see Figs. 10 and 11, and Sections 4.1.1-4.1.2), the presence of the surrounding strongly reduces the peak pressure coefficients on the lower part of the Cathedral flank (with decrements of about 50 to 70%), slightly increases them (up to about 10%) in the upper part of the lateral walls and on the transept façade, and remarkably intensifies the load on the roof (+15 to 25% in the central band).

Though not reported in Fig. 14, it is worth noting that the pressure fluctuations are such that the minimum coefficients on the windward side of the Cathedral often reach negative values (nearly everywhere in the configuration with surrounding buildings).

Given the possible vulnerability of large Gothic rose window, as highlighted by Soissons's recent disaster mentioned in the Introduction, the pressures acting on the great roses of the transept have been integrated at each time instant to account for the non-perfect simultaneity of the fluctuations, thus estimating a resulting force coefficient  $C_D$ .

The center of the rose windows is at a height above the ground of 25.8 m, and these have a surface area of about 85 m<sup>2</sup>. A specific set of measurements has been used to this purpose, where the two facades of the transept are finely instrumented. Specifically, the pressure field on the rose windows is discretized with 30 pressure taps. The resulting time histories are shown in Fig. 15 for the wind directions perpendicular to the transept façade (90° and 270°). It is apparent that the maximum load is obtained in the case without

surrounding for the windward window (Fig. 15(a); the nondimensional mean thrust is 0.82, while the peak value is 2.17). The load reduces by about 40% when the surrounding portion of the city is modeled and the wind blows from North-Northeast (Fig. 15(c), 90°-wind direction), due to the sheltering effect of the buildings very close to the Cathedral. Nevertheless, the load reduction is only 13% when the wind comes from South-Southwest (Fig. 15(d), 270°-wind direction) due to larger distance of the surrounding buildings. The leeward window is less loaded, and the resulting mean suction in the presence of the surrounding model is nearly the same as without surrounding (Fig. 15(b)) for the 270°-wind direction ( $\bar{C}_D = -0.43$ ), while a remarkable reduction is observed for the 90°-wind direction ( $\bar{C}_D = -0.34$ ). On the other hand, on the windward rose window load fluctuation increases in the presence of the surrounding model, and the peak force even becomes the same as in the case of a generic urban wind profile for a wind direction of 270° (Fig. 15(d),  $C_{D,max} = 2.15$ ).

## 5 Discussion

### 5.1 General considerations

The results reported in the previous section revealed that the Cathedral's geometrical complexity reflects on the measured pressure field. Apart from the remarkable peculiarity of the apse and the main façade of the Cathedral, for the sake of simplification one may say that the Cathedral of Notre Dame is a long construction with a depth discontinuously varying with the height (see the schematics in Fig. 16), so that the height-to-depth ratio is small (close to 1) considering the lower part of the church but significantly higher (about 2.3) referring to the top of the vertical walls. Also, the roof presents a high pitch (about

55°), and there are several other architectural elements (such as the jutting out body of the transept, the large flying buttresses, the balustrade at the base of the roof, or the various orders of gables) that are supposed to significantly influence the aerodynamic behavior of the construction. It is clear that the urban integration of the structure also plays a key role.

From the practical engineering standpoint, however, it is important to understand if all the specific aerodynamic features of a large Gothic Cathedral lead to significantly different wind loads for design or safety verification purposes compared to a more-or-less ordinary building. It is also to be noticed that only canonical wind velocity directions have been analyzed so far (those parallel or perpendicular to the Cathedral’s symmetry plane), while all possible wind directions must be considered instead for engineering purposes. Bearing in mind all these aspects, in the next section the load envelopes obtained for the finely-instrumented representative portion of the flank of the Cathedral (see Section 4.1.1) are compared with the few data available in the literature and with the loads proposed by Eurocode 1 for standard buildings.

## 5.2 Comparison with load models available in the literature

The mean pressure coefficients obtained for the finely instrumented portion of the flank of the Cathedral and the roof (Section 4.1.1) were averaged along the direction parallel to the longitudinal axis of the Cathedral (i.e., along the width of the considered Cathedral “slice”). Moreover, to comply with the prescriptions of Eurocode 1 (CEN 2004), the envelope pressure coefficients were calculated at any height above the ground for wind azimuths between  $-45^\circ$  and  $+45^\circ$  around the direction perpendicular to one of the Cathedral’s flanks. Results are reported in Fig. 16. It is noteworthy that, in the case of a generic

urban wind profile (without surrounding), the maximum mean pressure coefficient on the windward side is obtained for small or null skewness of the wind direction with respect to the canonical azimuths (either  $90^\circ$  or  $270^\circ$ ); therefore, the results for a wind perpendicular to the lateral walls represent a good estimate of the worst load case. In contrast, for the leeward side, the canonical wind directions provide nearly the lower load, whereas the higher suctions are obtained for inclinations of about  $45^\circ$  with respect to them. Clearly, results are more complicated and rather different for two flanks of the Cathedral when the surrounding buildings are modeled.

The comparison of the results for the configurations with and without surrounding emphasizes the importance of modeling the buildings, the river and the other details of the city around the Cathedral. As expected, for the case without surrounding, both windward and leeward pressure coefficient envelopes on the right and left sides of the Cathedral are nearly identical. On the windward side, in the presence of the surrounding model, the pressure coefficient envelope exhibits significantly lower values in the inferior part of the walls (with reductions up to about 60-70%) when one considers the left flank of the Cathedral (then, when the wind direction is between  $45^\circ$  and  $135^\circ$ , and the buildings are close to the church; see Fig. 5). In contrast, on the right flank (then, if the wind blows from directions  $225^\circ$  and  $315^\circ$ ), the pressure coefficients are very similar to the case without surrounding in the lower part of the walls. For a height above the ground between about  $0.6H$  and  $0.75H$ , the windward pressure envelopes for the left and right flanks of the Cathedral become fairly close and non-negligibly higher than the case without surrounding (with increments up to nearly 20%). As for the leeward pressure coefficient envelopes, the suction is lower if the surrounding buildings are modeled; in particular, the difference is on average of 12 and 17% for the left and right side of the Cathedral,

respectively.

The measured pressure coefficients on the windward side of the considered part of the Cathedral are generally lower (or even much lower in some regions) than the values suggested by Eurocode 1, except for a small portion of the roof for the case with surrounding. In contrast, on the leeward side the measured pressures tend to be slightly lower (higher suction) on the vertical walls of the Cathedral and significantly lower on the roof, especially for the configuration without surrounding. In particular, for a generic urban boundary layer flow, the integral mean normal force coefficient acting on the windward side of the roof results to be more than 30% lower than Eurocode 1's prescriptions, whereas that acting on the leeward side is more than double. Consequently, both the resulting drag and uplifting forces are increased. The same effects are also observed if the buildings surrounding the Cathedral are modeled, but the decrease/increase of the windward/leeward normalized forces are less pronounced. Finally, the experimental data by Mark and Jonash (1970) for a Cathedral-like construction are in agreement with the pressure coefficient envelopes in the lower part of the windward vertical walls for the case of a generic urban boundary layer, while they overestimate the loads in the upper part. In contrast, on the leeward side these literature data underestimate the suction on most part of the vertical walls, but they overestimate it in the top part.

Considering again the large roses of the transept (see Fig. 15), one can remark that the mean load without surrounding on the windward window is in line with the prescriptions of Eurocode 1 (Fig. 16), provided that the velocity pressure at the top of the roof is used to normalize the force or the pressure coefficient (which is not the only option in Eurocode 1). The gust factor (ratio of peak to mean load) for the windward rose perfectly complies with the value suggested by Eurocode 1 (slightly less than 2.2) based on the turbulence

intensity in the approaching wind profile at the height of the window. In contrast, it is higher in the presence of the surrounding buildings (larger than 3). However, it is very important to stress that the canonical wind directions (either  $90^\circ$  or  $270^\circ$ ) considered in the analysis of the load on the rose windows (see Fig. 15) do not always represent the worst case scenario, especially for negative pressures on the leeward side, as it has already been emphasized for the finely instrumented portion of the flank of the Cathedral. In particular, mean suction forces as low as  $-0.63$  (for a wind direction of either  $135^\circ$  or  $225^\circ$ ) and  $-0.73$  (for a wind direction of  $130^\circ$ ) have been obtained for the cases without and with surrounding, respectively.

Finally, one can notice that the effective load acting on most parts of the Cathedral will also depend on the internal pressures, which have not been investigated in the present work. Their estimation is a very complicated task as it requires the accurate modeling of diffused openings all over the building. However, in the absence of dominant openings (produced, for instance, by the failure of a window), for structural verifications it may be reasonable to consider the standard range  $-0.3$  to  $+0.2$  recommended by Eurocode 1 (CEN 2004).

## 6 Conclusions

The results of the wide wind tunnel test campaign that has been carried out on a scale model of the Cathedral of Notre Dame in Paris led to some major conclusions, reported hereafter.

Firstly, the complex geometry of a large Gothic cathedral, both in the aerial projection and in elevation, as well as the important aerodynamic role played by some architectural elements imply specific phenomena in the wind-structure interaction process that do not

allow the correct estimation of the wind loads based on the data available for standard buildings. Specifically, the present results reveal that, depending on the structural element considered or the specific configuration examined, these loads can be either significantly higher or lower than the values that can be predicted based on codes and standards. In particular, the roof of the Cathedral may be subjected to drag and uplifting forces significantly larger than those calculated with the Eurocode 1, which demonstrates the need for accurate wind tunnel tests to assess the safety of this type of structures.

Secondly, the influence on the wind load of the neighboring portion of the city where the considered Cathedral stands is extremely important, and can vary on a case-by-case basis. The current analysis highlights that the presence of the surrounding buildings does not only affect the aerodynamics of the portions of the Cathedral at a comparable height but also of parts significantly above. For instance, the drag force on the roof of the Cathedral increases by nearly 10%, while the uplifting force reduces to about one third. For the large rose windows of the transept, another potentially sensitive element of the Cathedral, the behavior is more complicated; indeed, the modeling of the neighboring portion of the city implies a lower mean thrust force but also a rise of the load fluctuations.

The results reported in the current paper may represent a guideline to determine the wind load on complex buildings such as Gothic Cathedrals. Nevertheless, once the wind climate in the city of Paris has accurately been evaluated, the nondimensional pressure coefficients presented herein can be transformed in loads and used to assess the structural safety of the Cathedral of Notre Dame, in a similar way to the analysis carried out by Vannucci et al. (2019). Therefore, this work may represent a first step towards the goal of guaranteeing the wind safety of architectural treasures like Gothic Cathedrals, even if in the future heavier and heavier effects of climate change are likely to occur.

## Acknowledgments

Authors want to thank:

- Martin Peters, former director of the Eiffel Wind Tunnel Laboratory, Paris, for his valuable help concerning the history of wind tunnel research on historical monuments.
- Emmanuel Portet and Laure Frèrejean, University of Versailles and Saint Quentin, for their fruitful commitment and help in the administrative and financial aspects of this research.
- Bernardo Nicese, Clara Gessl and Petar Melnjak, who helped us in the execution of the laboratory tests in Prato.

## References

- 3D CAD browser (2021). [www.3dcadbrowser.com](http://www.3dcadbrowser.com).
- 3D Warehouse (2014). Notre Dame de Paris.  
<https://3dwarehouse.sketchup.com/model/cf5038cd918ff49c63995fb119e59971/Notre-Dame-de-Paris>.
- Blender Online Community (2021). *Blender - a 3D modelling and rendering package (release 3.0)*. Stichting Blender Foundation, Amsterdam: Blender Foundation.
- Blocken, B. (2014). 50 years of computational wind engineering: Past, present and future. *Journal of Wind Engineering and Industrial Aerodynamics* 129, 69–102.
- Borri, C. and L. Facchini (1999). Wind induced loads on the monumental roof structure of the XII century, Palazzo della Ragione, in Padova. In *Proc. of 10th ICWE (International*



*Conference on Wind Engineering), Copenhagen, Volume II, Rotterdam, Denmark, pp.*  
1105–1111. Balkema A. A.

Brocato, M., I. Stefanou, P. Vannucci, C. Coulangeon, M. Ferrucci, F. Pantalone, E. De-  
chorgnat, F. Oran, A. Pallard, J. Pellerin, A. Diao, M. Kun, and A. A. Albero (2016).  
AVACAT, Analyse de vulnérabilité de l’architecture capétienne face aux tempêtes.  
Technical report, ENSA Paris-Malaquais, Laboratoire GSA.

Calderini, C. and L. C. Pagnini (2015). The debate on the strengthening of two slen-  
der masonry structures in early xx century: A contribution to the history of wind  
engineering. *Journal of Wind Engineering and Industrial Aerodynamics* 147, 302–319.

Cano-Vicent, A., M. M. Tambuwala, S. S. Hassan, D. Barh, A. A. A. Aljabali, M. Birkett,  
A. Arjunan, and A. Serrano-Aroca (2021). Fused deposition modelling: Current status,  
methodology, applications and future prospects. *Additive Manufacturing* 47, 102378.

CEN, E. C. f. S. (2004). EN 1991-1-4, Eurocode 1: Part 4: wind actions.

Chien, N., Y. Feng, H. H. Want, and T. T. Siao (1951). Wind tunnel studies of pressure  
distribution on elementary building forms. Technical report, Institute of Hydraulics  
Research, University of Iowa, Ames, Iowa.

Coccia, S., M. Como, and F. D. Carlo (2015). Wind strength of Gothic Cathedrals.  
*Engineering Failure Analysis* 55, 1–25.

Como, M. (2013). *Statics of historic masonry constructions*. Berlin, Germany: Springer  
Verlag.

Davenport, A. G. (1961). The application of statistical concepts to the wind loading of  
structures. *Proceedings of the Institution of Civil Engineers* 19(4), 449–472.

630 Deland, T. T., M. Sadegh, and K. T. Sina (2020). The semantic conservation of architec-  
631 tural heritage: the missing values. *Heritage Science* 8, 70.

632 Domede, N., L. Pena, and N. Fady (2019). Historical review of lighthouse design under  
633 wind load: the Ile Vierge lighthouse. *Philosophical Transactions of the Royal Society*  
634 *A: Mathematical, Physical and Engineering Sciences* 377(2155), 20190167.

635 Ferrucci, M. and M. Peter (2020). La puissance de la recherche inconsciente: cent ans  
636 d’expérimentation aérodynamique à la soufflerie eiffel. In *Architecture et Expérimenta-*  
637 *tion*, pp. 44–75. Rouen, France: ATE - Editions des Méandres.

638 Holmes, J. D. (1997). Equivalent time averaging in wind engineering. *Journal of Wind*  
639 *Engineering and Industrial Aerodynamics* 72, 411–419.

640 Holmes, J. D. (2007). *Wind Loading of Structures* (second ed.). CRC Press.

641 Irwin, H. P. A. H., K. R. Cooper, and R. Girard (1979). Correction of distortion ef-  
642 fects caused by tubing systems in measurements of fluctuating pressures. *Journal of*  
643 *Industrial Aerodynamics* 5, 93–107.

644 Lawson, T. V. (1976). The design of cladding. *Building and Environment* 11, 37–38.

645 Lynxter (2021). Industrial multi-materials 3D printer S600D.  
646 <https://lynxter.fr/en/product/professional-industrial-3d-printers/>.

647 Mark, R. (1982). *Experiments in gothic structure*. Cambridge, Massachussets: MIT Press.

648 Mark, R. (1984). *High gothic structure - A technological reinterpretation*. Princeton, New  
649 Jersey: Princeton University Press.

650 Mark, R. and R. S. Jonash (1970, 10). Wind Loading on Gothic Structure. *Journal of*  
651 *the Society of Architectural Historians* 29(3), 222–230.

652 MiniWorld3D (2019). Notre-Dame de Paris Cathedral.

653 [https://www.myminifactory.com/object/3d-print-notre-dame-de-paris-cathedral-](https://www.myminifactory.com/object/3d-print-notre-dame-de-paris-cathedral-91899)

654 91899.

655 Mitchell, A., U. Lafont, M. Hołyńska, and C. Semprimoschnig (2018). Additive manufac-

656 turing — a review of 4d printing and future applications. *Additive Manufacturing* 24,

657 606–626.

658 Ngo, T. D., A. Kashani, G. Imbalzano, K. T. Nguyen, and D. Hui (2018). Additive man-

659 ufacturing (3d printing): A review of materials, methods, applications and challenges.

660 *Composites Part B: Engineering* 143, 172–196.

661 OpenStreetMap (2017). Map of Paris. <https://www.openstreetmap.org> .

662 Orr, S. A., J. Richards, and S. Fatorić (2021). Climate change and cultural heritage: A

663 systematic literature review (2016–2020). *The Historic Environment: Policy & Prac-*

664 *tice* 0(0), 1–43.

665 Romani, L. (1972). Rouen, Place du Vieux Marché, Efforts du vent sur l’église (mesures

666 en soufflerie). Technical report, Laboratoire Aérodynamique Eiffel.

667 Simiu, E. and D. Yeo (2019). *Wind Effects on Structures - Modern Structural Design for*

668 *Wind* (fourth ed.). Wiley Blackwell.

669 Simplify3D (2021). All-In-One 3D Printing Software - Simplify3D software.

670 <https://www.simplify3d.com/>.

671 Solari, G., T. A. Reinhold, and F. Livesey (1998). Investigation of wind actions and effects

672 on the Leaning Tower of Pisa. *Wind and Structures* 1 (1), 1–23.

673 Steenbergen, R. D. J. M., T. Koster, and C. P. W. Geurts (2012). The effect of cli-  
674 mate change and natural variability on wind loading values for buildings. *Building and*  
675 *Environment* 55, 178–186.

676 Szalay, Z. (1983). Wind loads on an ancient church spire. *Journal of Wind Engineering*  
677 *and Industrial Aerodynamics* 11(1), 187–199.

678 Ungewitter, G. G. (1890). *Lehrbuch der Gotischen Konstruktionen*. Leipzig, Germany.  
679 Available at Biblioteca Meccanico Architettonica: <http://www.bma.arch.unige.it>: T.  
680 O. Weigel Nachfolger.

681 Vannucci, P. (2021). A study on the structural functioning of the ancient charpente of  
682 Notre-Dame, with a historical perspective. *Journal of Cultural Heritage* 49, 123–139.

683 Vannucci, P., F. Masi, and I. Stefanou (2019). A nonlinear approach to the wind strength  
684 of Gothic Cathedrals: The case of Notre Dame of Paris. *Engineering Structures* 183,  
685 860–873.

686 Wang, X., M. Jiang, Z. Zhou, J. Gou, and D. Hui (2017). 3D printing of polymer matrix  
687 composites: A review and prospective. *Composites Part B: Engineering* 110, 442–458.

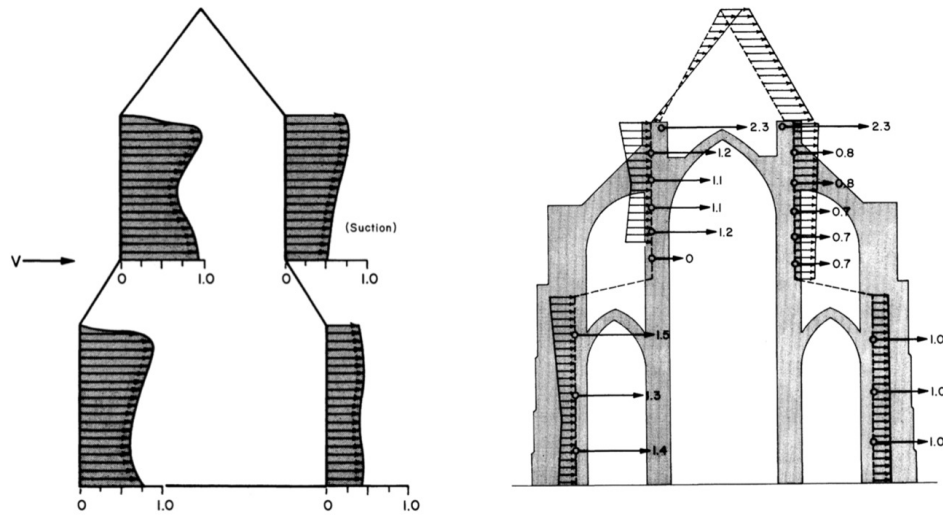


Figure 1: The wind pressure coefficients as experimentally measured in [Chien et al. \(1951\)](#), left, and how they are applied to a bi-dimensional Cathedral model in [Mark and Jonash \(1970\)](#), right.

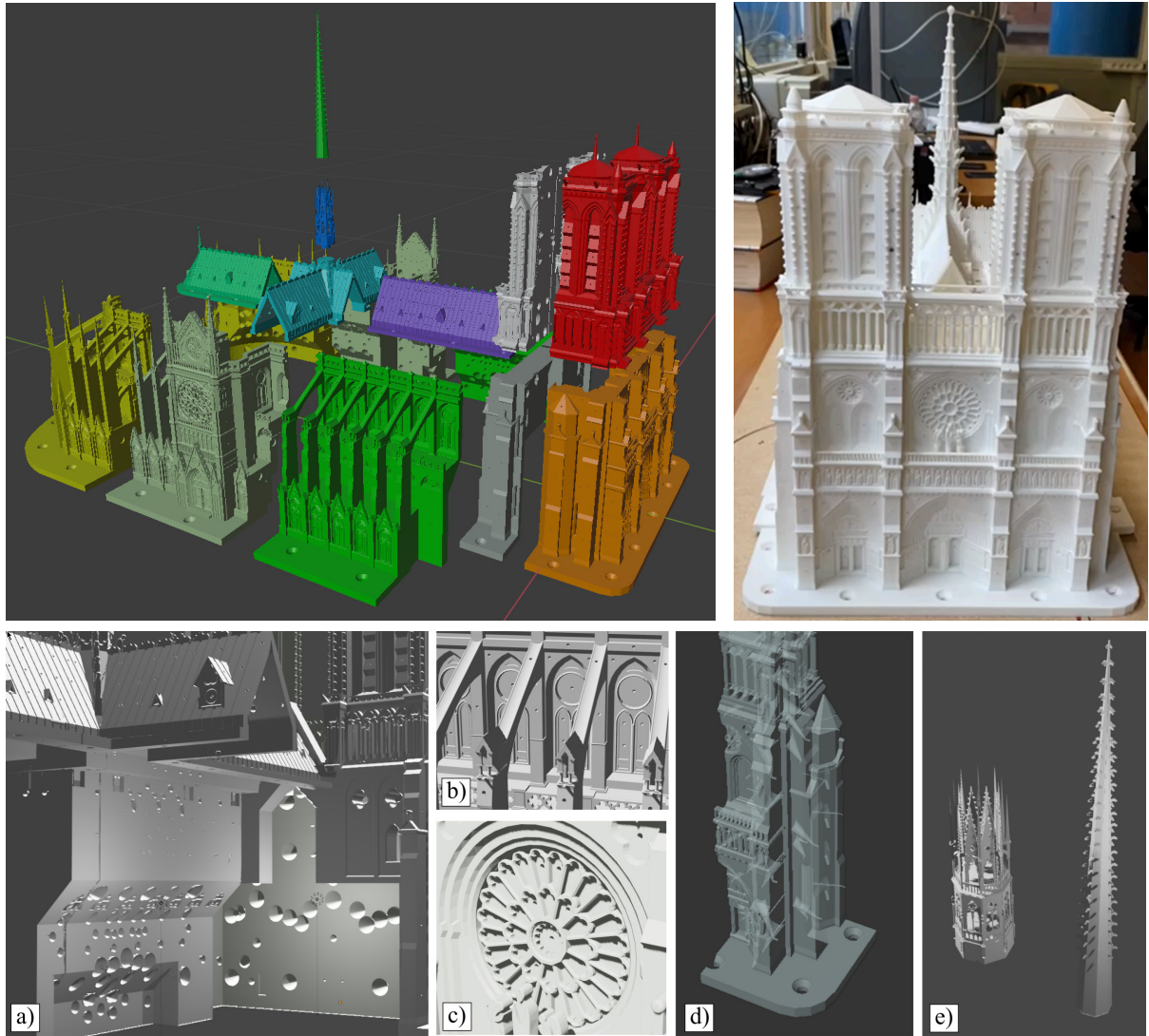


Figure 2: The Cathedral model: top, left: the 15 parts of the numerical model; right: the fabricated model; bottom: a) detail of the internal volume (façade and nave) with the conical holes to place the pressure tubes; b) detail of the external surface of the nave; c) detail of the rose on the façade; d) internal view of a portion of the façade; e) spire model split into two parts.

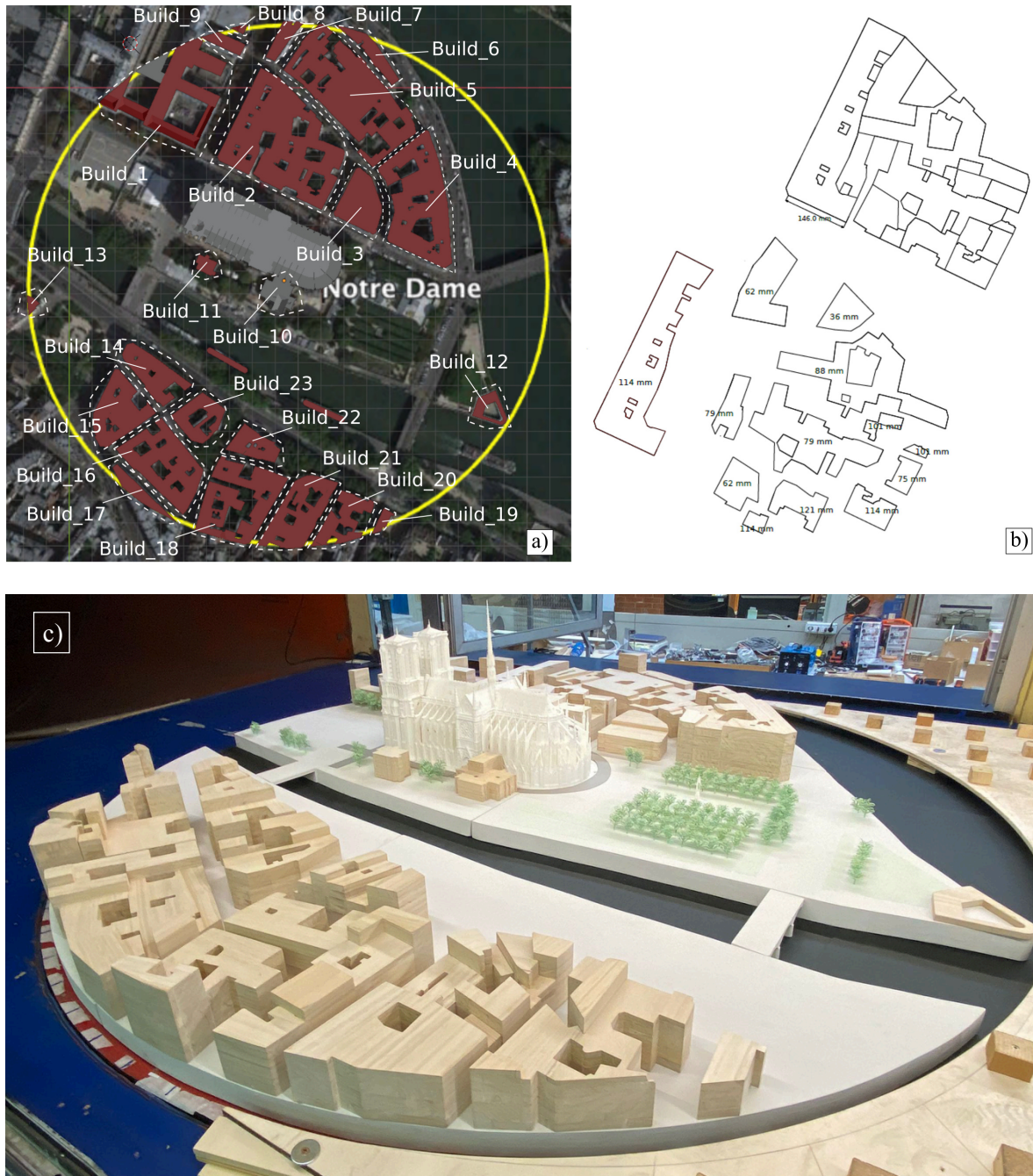


Figure 3: Model of the surrounding of the Cathedral; a) selected blocks of buildings for the model; b) example of a planform with the internal building partitions; c) view of surrounding and Cathedral models mounted on the turning table in the wind tunnel.



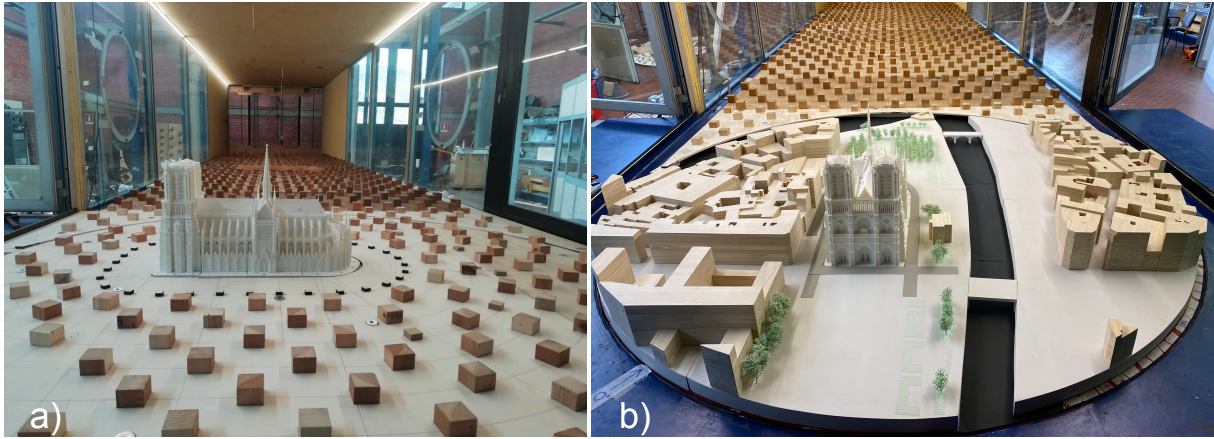


Figure 4: Model of the Cathedral in the wind tunnel: a) without and b) with surrounding.

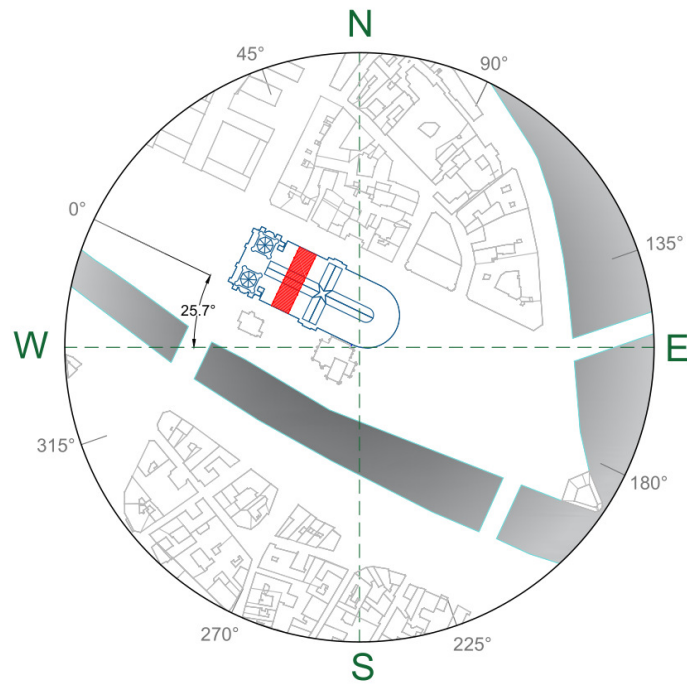
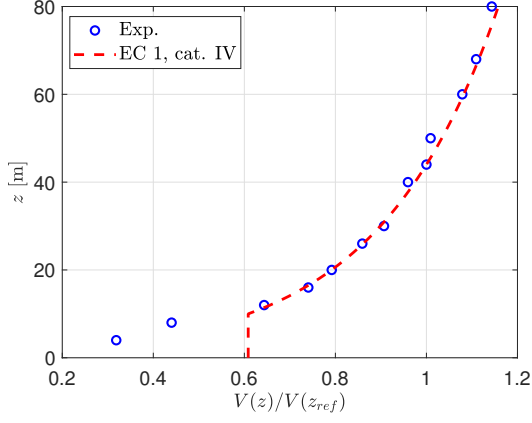


Figure 5: Scheme indicating the wind directions with respect to the Cathedral (the 0°-direction is perpendicular to the front of the building). The portion of the flank of the Cathedral that has been studied in detail in Section 4.1.1 is highlighted in red.

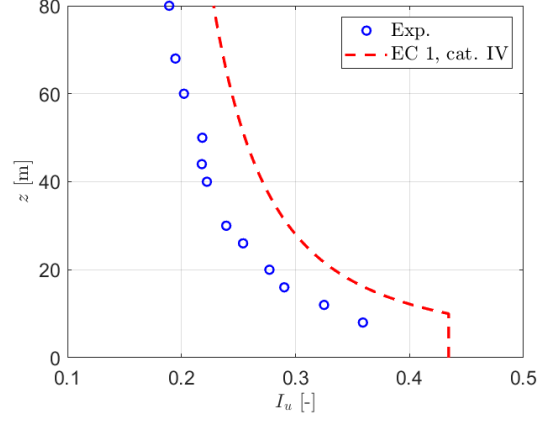




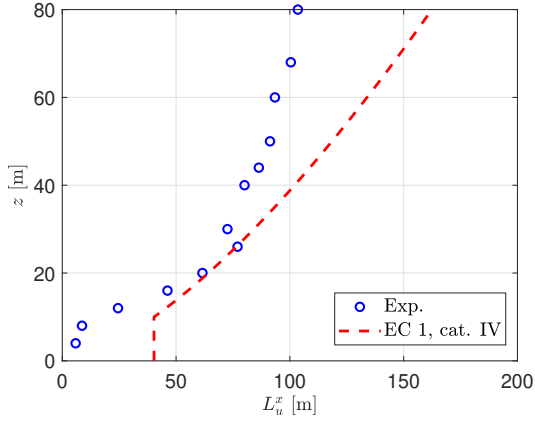
Figure 6: Parts of the model equipped with pressure taps; the Teflon tubes are connected to an ESP pressure scanner (the black box visible at the bottom).



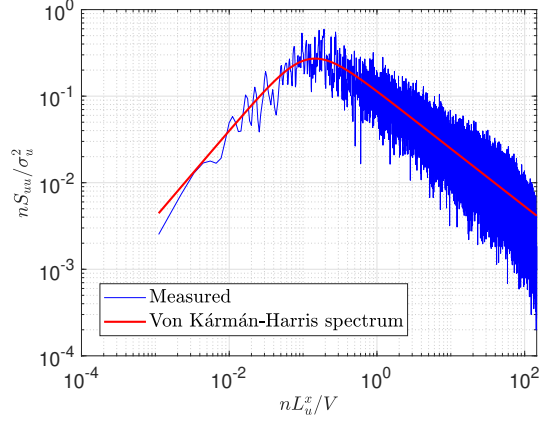
(a)



(b)



(c)



(d)

Figure 7: (a) Normalized mean velocity ( $z_{ref} = H = 44$  m denotes the reference height, i.e., the top of the roof), (b) turbulence intensity, and (c) longitudinal integral length scale of turbulence profiles in the present tests. The power spectral density of longitudinal velocity fluctuations at the reference height is shown too (d).

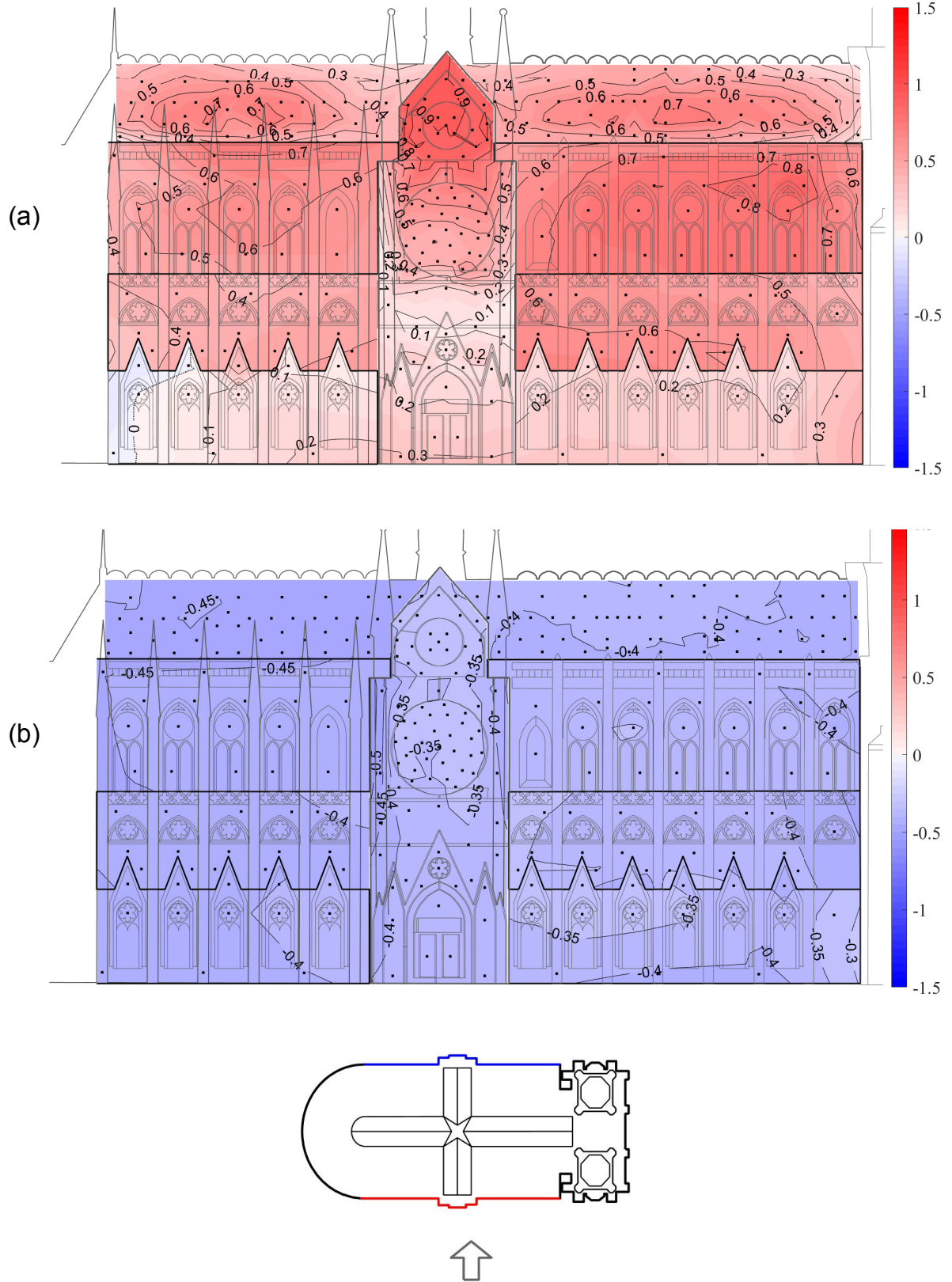


Figure 8: Mean pressure coefficient distribution on the flank of the Cathedral for the configuration with surrounding: windward side (a) and leeward side (b). The wind velocity direction is sketched at the bottom (from North-Northeast, perpendicular to the side walls and denoted as  $90^\circ$  in Fig. 5).

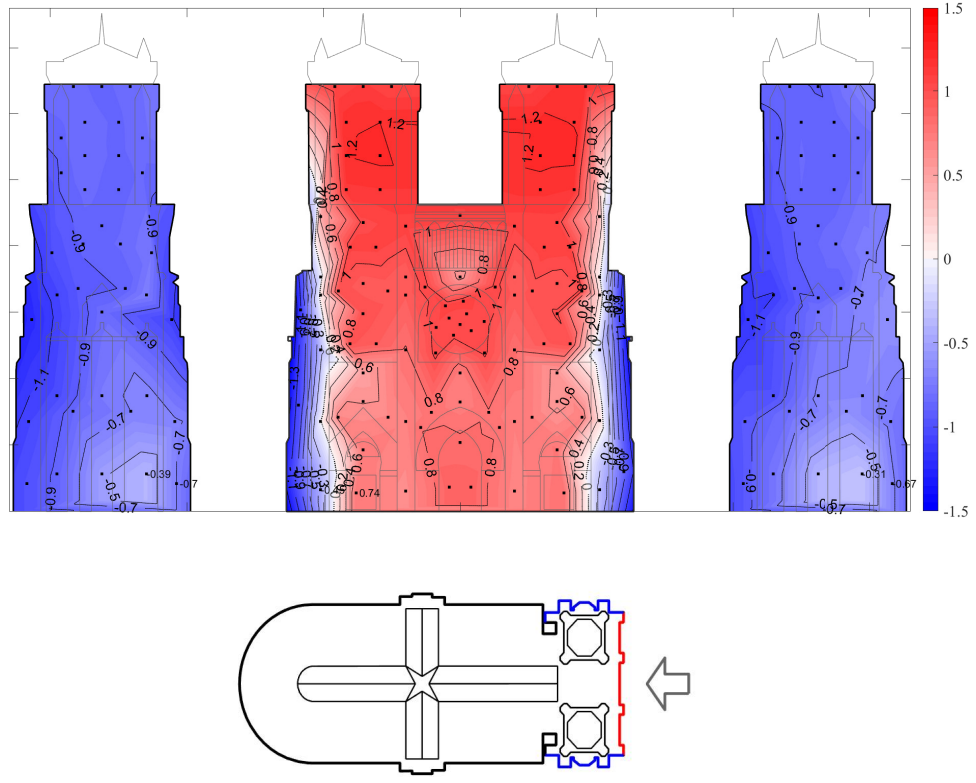


Figure 9: Mean pressure coefficient distribution on the front of the Cathedral and on the external sides of the towers for the configuration with surrounding. The wind velocity direction is sketched at the bottom (from West-Northwest, perpendicular to the main façade and denoted as  $0^\circ$  in Fig. 5).

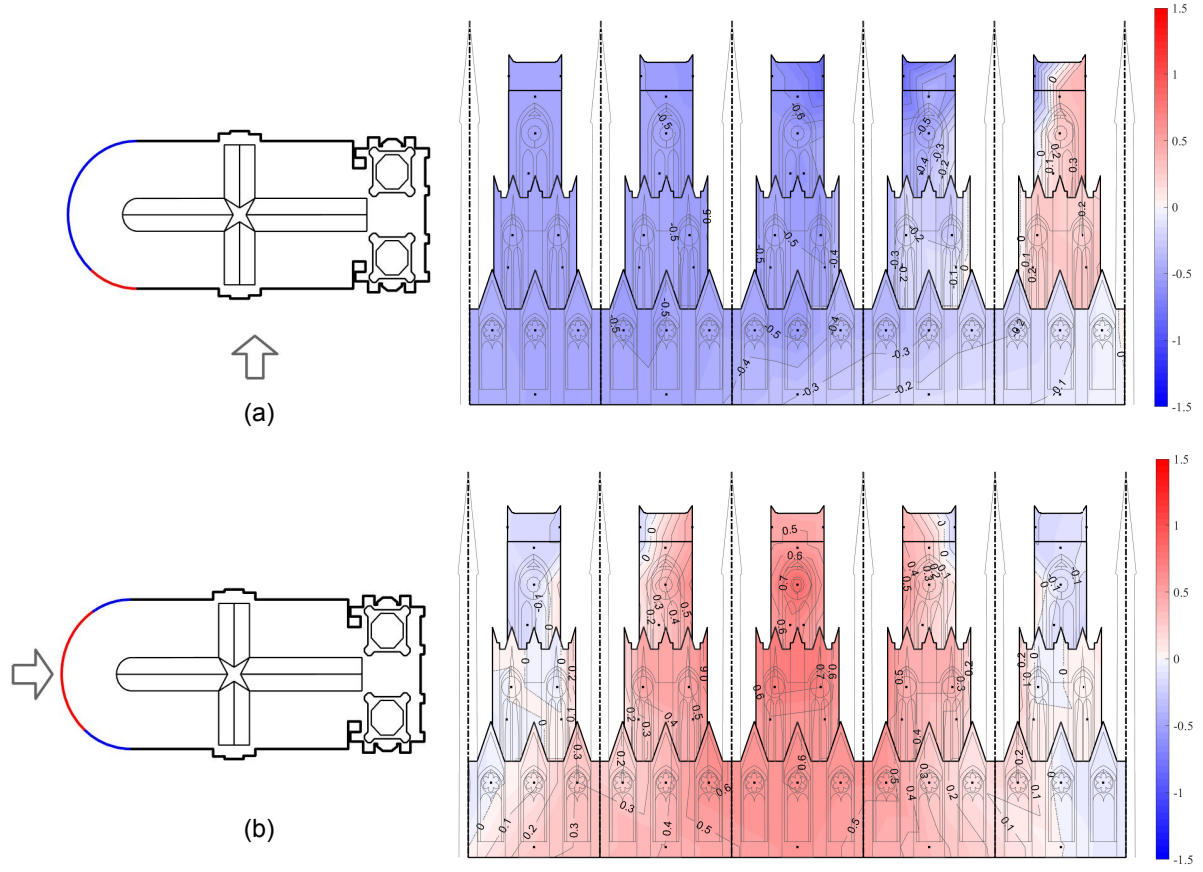


Figure 10: Mean pressure coefficient distribution on the development of the apse of the Cathedral (the curved surface of the Cathedral is unrolled on a plane) for the configuration with surrounding: wind velocity directions of 90° (a) and 180° (b).

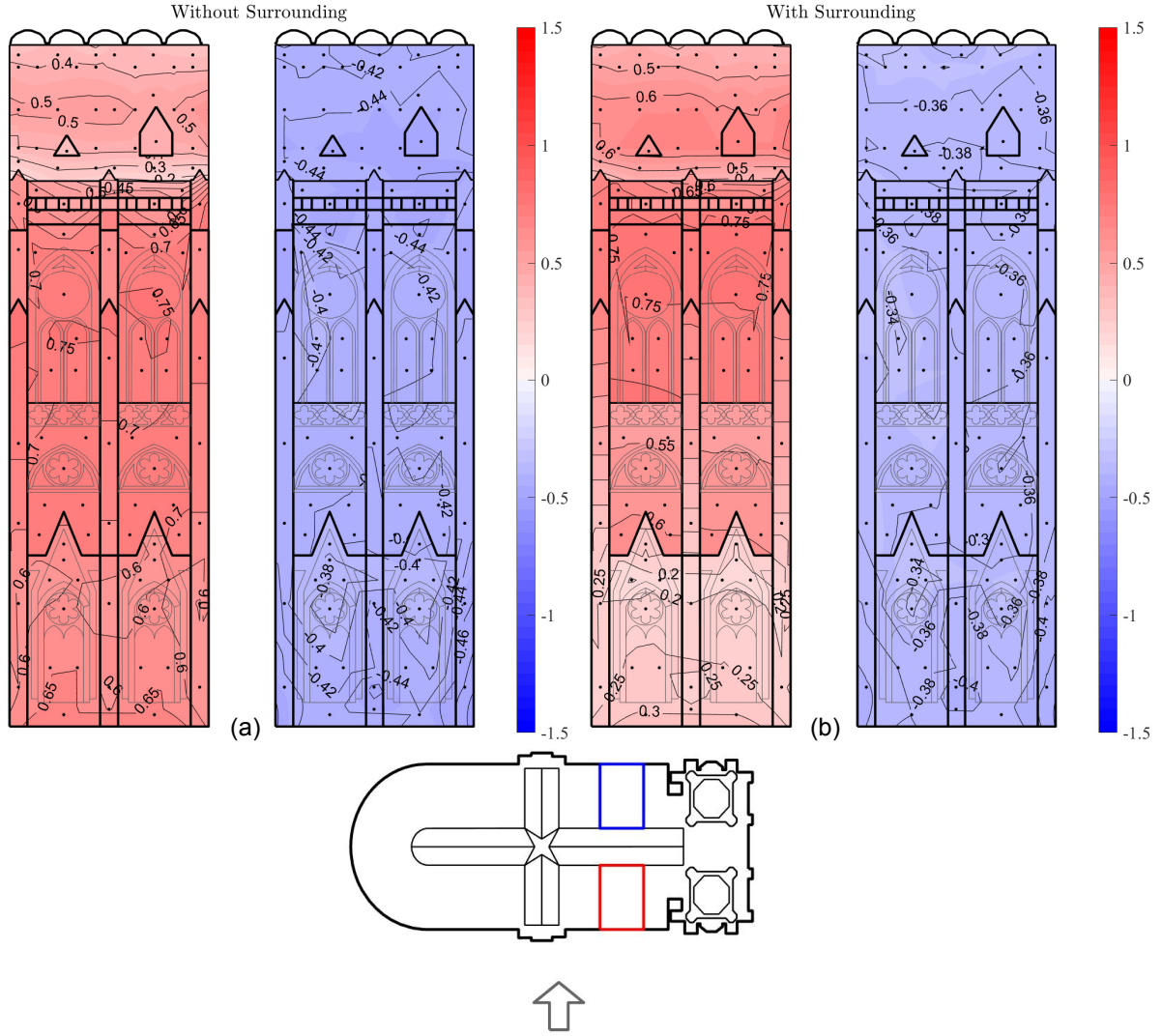


Figure 11: Mean pressure coefficient distribution on a lateral portion of the Cathedral (see Fig. 5) for the configuration without the model of the surrounding (a) and including the buildings around the Cathedral (b). Each frame reports on the left the windward side and on the right the leeward side. The wind velocity direction is sketched at the bottom (perpendicular to the North-Northeast flank, denoted as  $90^\circ$  in Fig. 5).



Figure 12: Flow visualization with a smoke generator in the roof region. The wind direction is perpendicular to the flank of the Cathedral ( $90^\circ$ ).



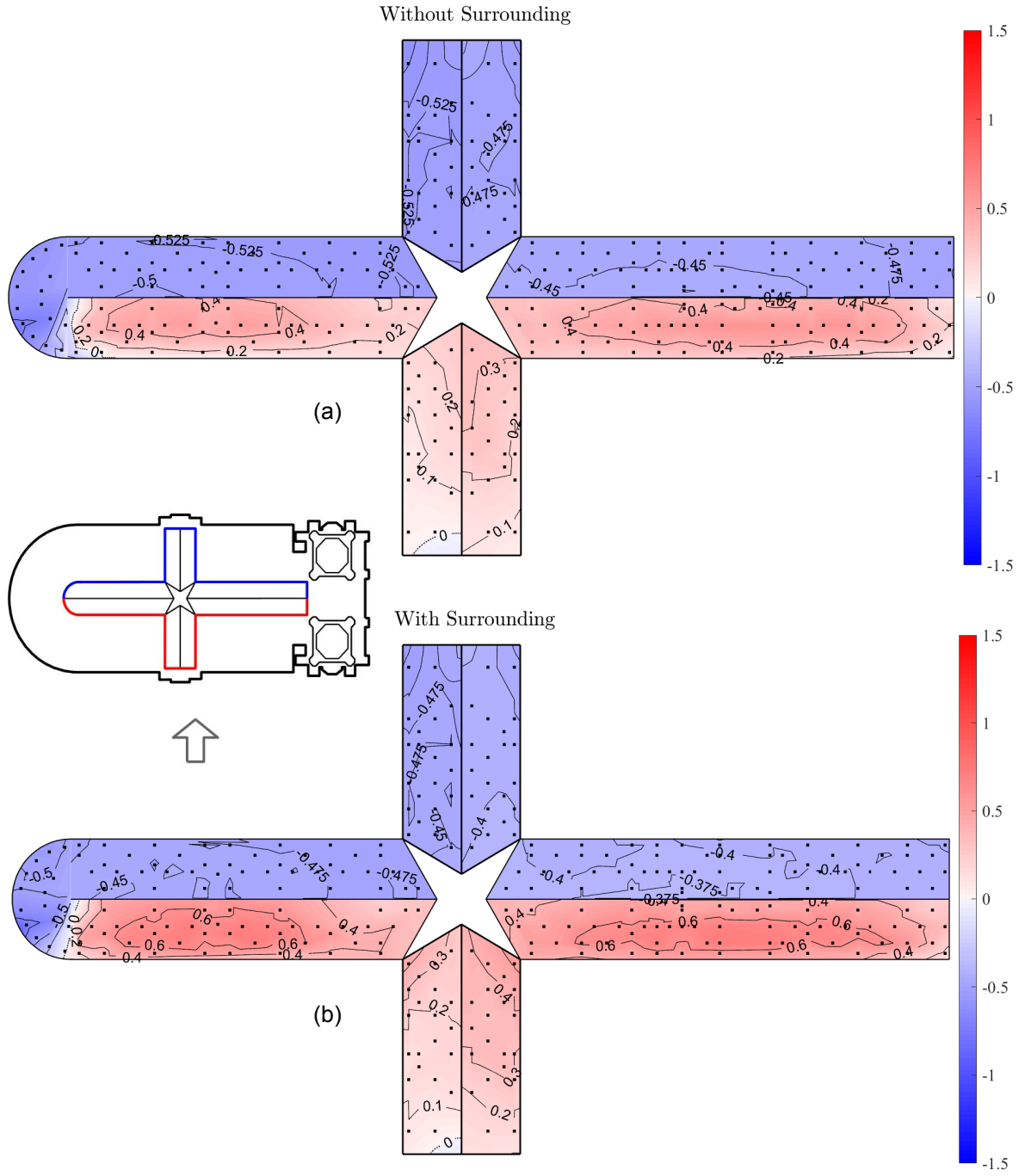


Figure 13: Plan view of the mean pressure coefficients on the roof of the Cathedral: results without surrounding (a) and with surrounding (b). The wind direction, also sketched, is that denoted as  $90^\circ$  in Fig. 5.



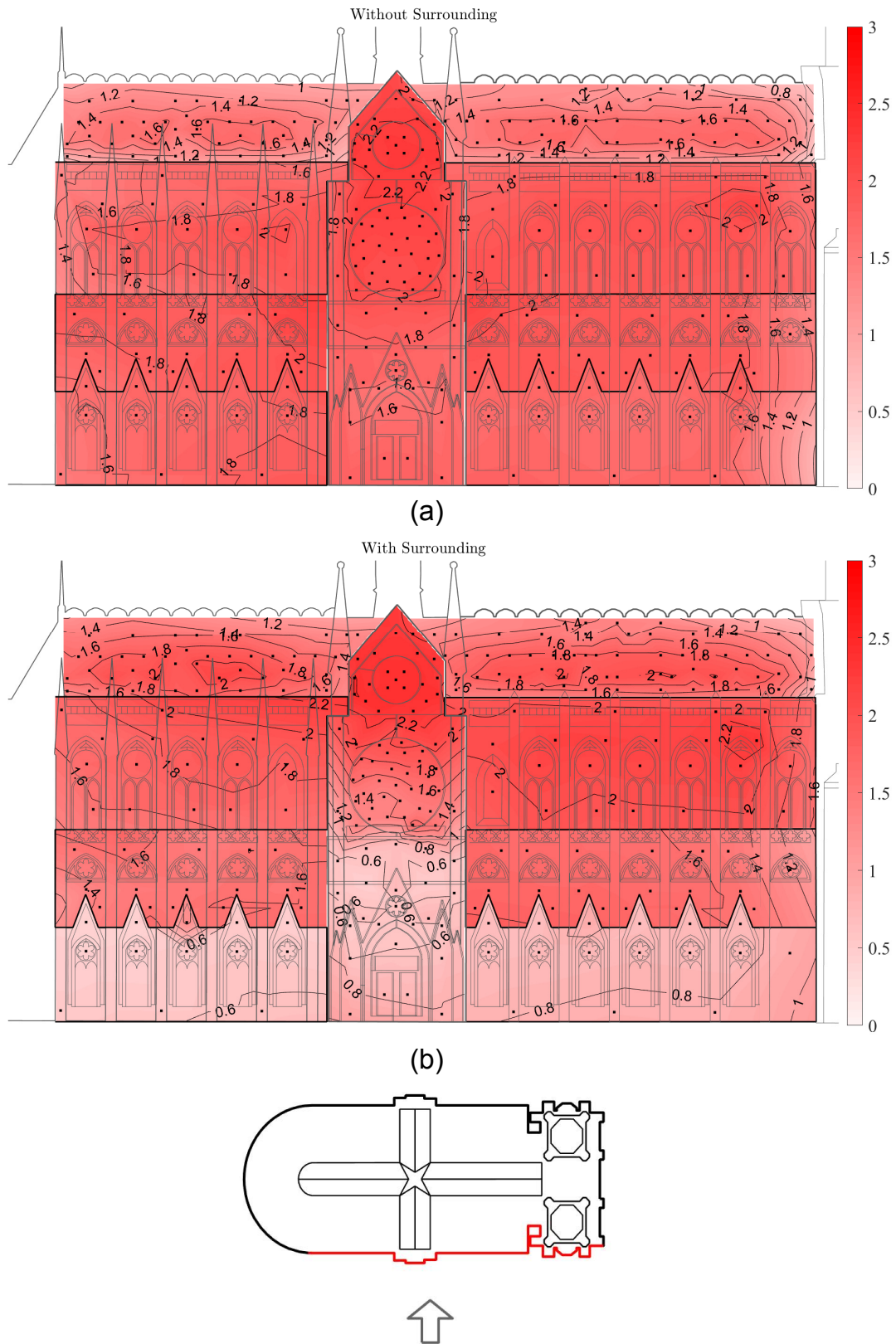


Figure 14: Distribution of the maximum pressure coefficients on the windward flank of the Cathedral for a wind direction perpendicular to it ( $90^\circ$ , sketched at the bottom): configuration without surrounding (a) and with surrounding (b).

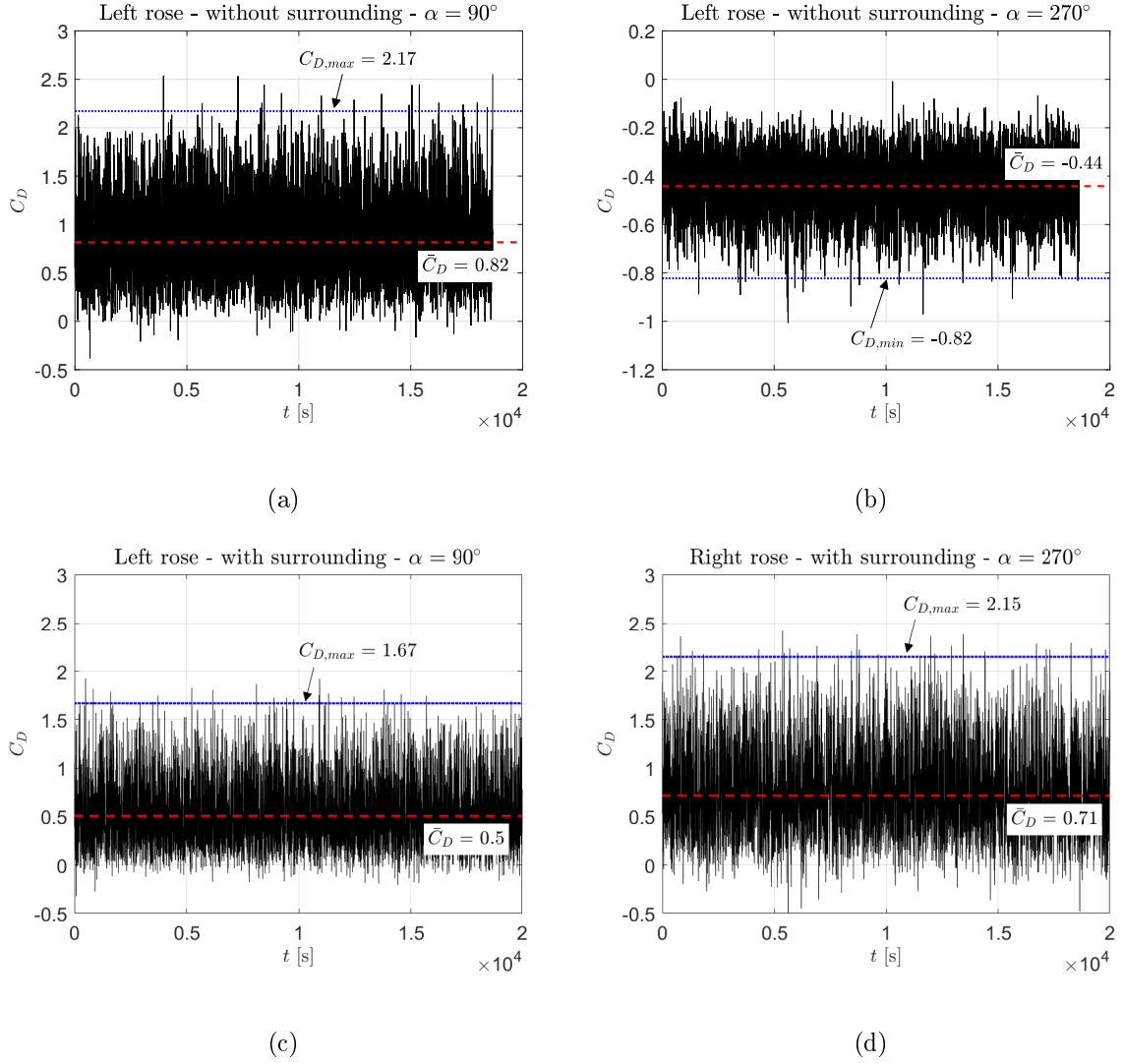


Figure 15: Time history of the integrated force coefficient ( $C_D = A^{-1} \int_A C_p dA$ , where  $A$  denotes the area of the window; time refers to full scale) on the great rose windows of the transept: (a) left rose, wind direction  $90^\circ$ , without surrounding buildings; (b) left rose, wind direction  $270^\circ$ , without surrounding buildings; (c) left rose, wind direction  $90^\circ$ , with surrounding buildings; (d) right rose, wind direction  $270^\circ$ , with surrounding buildings. Both mean and peak values of the load coefficient are reported.

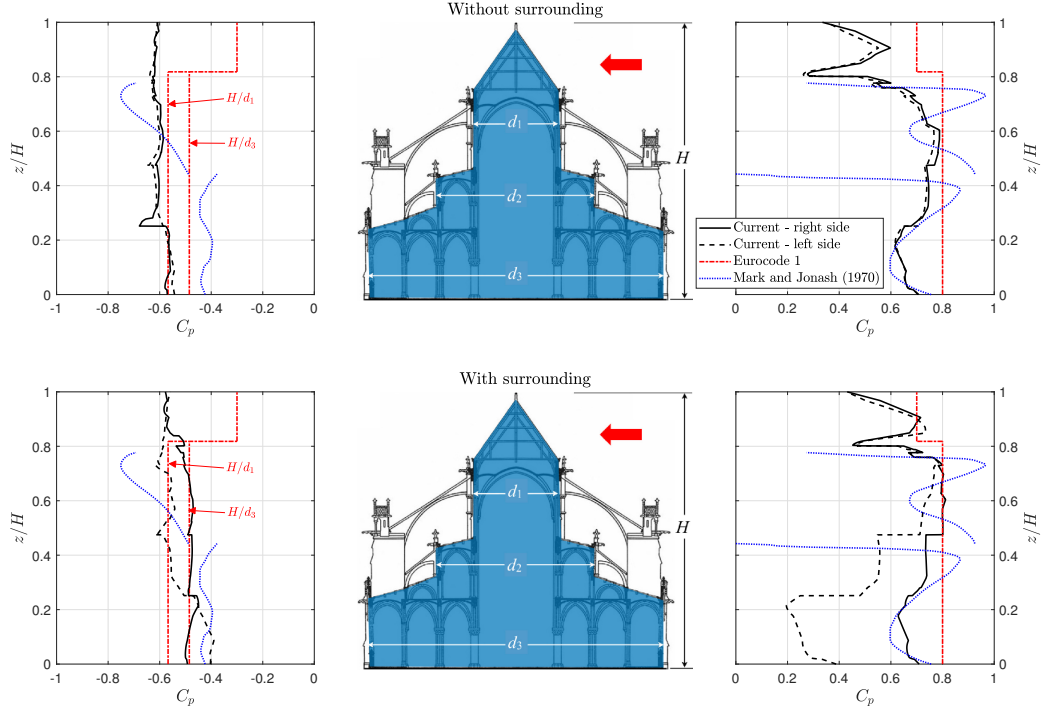


Figure 16: Envelope of mean pressure coefficients along a section of the Cathedral perpendicular to its longitudinal axis for the cases without (top) and with (bottom) surrounding buildings. Comparison with Eurocode 1 (CEN 2004) prescriptions for ordinary buildings and with the data adapted from Mark and Jonash (1970). Windward pressures are reported on the right of the figure, while leeward pressures can be read on the left. “right side” in the caption refers to the nominal wind direction indicated in the schematics (red arrow), whereas “left side” denotes the opposite wind direction.